Lithium-Catalyzed Dehydrogenation of Ammonia Borane within Mesoporous Carbon Framework for Chemical Hydrogen Storage

By *Li Li, Xiangdong Yao,* Chenghua Sun, Aijun Du, Lina Cheng, Zhonghua Zhu, Chengzhong Yu, Jin Zou, Sean C. Smith, Ping Wang, Hui-Ming Cheng, Ray L. Frost,* and *Gao Qing (Max) Lu**

Ammonia borane (AB) has attracted tremendous interest for on-board hydrogen storage due to its low molecular weight and high gravimetric hydrogen capacity below a moderate temperature. However, the slow kinetics, irreversibility, and formation of volatile materials (trace borazine and ammonia) limit its practical application. In this paper, a new catalytic strategy involved lithium (Li) catalysis and nanostructure confinement in mesoporous carbon (CMK-3) for the thermal decomposition of AB is developed. AB loaded on the 5% Li/CMK-3 framework releases ~7 wt % of hydrogen at a very low temperature (around 60 °C) and entirely suppresses borazine and ammonia emissions that are harmful for proton exchange membrane fuel cells. The possible mechanism for enhanced hydrogen release via catalyzed thermal decomposition of AB is discussed.

1. Introduction

On-board hydrogen storage is a major challenge for the commercialization of fuel cell vehicles.[1] The US Department of Energy (DOE) has set a target of 6 wt % hydrogen capacity at a range of operational temperatures (−30 ~ 80 °C) with fast kinetics for hydrogen storage. To meet the DOE target for on-board applications, hydrogen storage materials must have light weight and a high chemical weight percentage of hydrogen with a rapid hydrogen release rate below 80 °C, which then enables the utilization of the waste heat from a proton exchange membrane (PEM) fuel cell to release hydrogen from the storage materials.

Ammonia borane (AB), NH_3BH_3, has been considered as a promising candidate material for hydrogen storage due to its very large stoichiometric hydrogen content (~19.6 wt %), moderate temperatures for thermal decomposition, the exothermic nature of decomposition process, as well as the fact that it is inflammable and nonexplosive.[2] Recent thermoanalytical results have shown that AB releases hydrogen with three steps[3]:

$$NH_3BH_3 \rightarrow NH_2BH_2 + H_2 < 120\,^{\circ}C \quad (1)$$

$$NH_2BH_2 \rightarrow NHBH + H_2 > 120\,^{\circ}C \quad (2)$$

$$NHBH \rightarrow NB + H_2 > 500\,^{\circ}C \quad (3)$$

[*] Dr. X. D. Yao, Prof. G. Q. (Max) Lu, Dr. L. Li, Dr. C. H. Sun, Dr. A. J. Du, L. Cheng, Prof. S. C. Smith, Prof. Z. H. Zhu
ARC Centre of Excellence for Functional Nanomaterials
School of Engineering and Australian Institute of Bioengineering and Nanotechnology
The University of Queensland
QLD 4072 Brisbane (Australia)
E-mail: x.yao@uq.edu.au; maxlu@uq.edu.au
Dr. C. H. Sun, Dr. A. J. Du, Prof. S. C. Smith
Centre for Computational Molecular Science
The University of Queensland
QLD 4072 Brisbane (Australia)
Prof. C. Z. Yu
Department of Chemistry, Fudan University
Shanghai 200433 (P.R. China)
Dr. J. Zou
Centre for Microscopy and Microanalysis and School of Engineering
The University of Queensland
QLD 4072 Brisbane (Australia)
Dr. P. Wang, Prof. H. M. Cheng
Shenyang National Laboratory for Materials Science
Institute of Metal Research
Chinese Academy of Sciences
Shenyang 110016 (P.R. China)
Prof. R. L. Frost
School of Physical & Chemical Sciences
Queensland University of Technology
QLD 4001 Brisbane (Australia)

DOI: 10.1002/adfm.200801111

Reactions (1) and (2) stepwise releases 6.5 and 6.9 wt % of hydrogen below 200 °C, with the formation of polyaminobrane $(NH_2BH_2)_x$ and polyiminoborane $(NHBH)_x$, respectively. Reaction (3) releases 7.3 wt % of hydrogen, but is impractical for hydrogen storage because of the very high decomposition temperature (>500 °C). During the thermal decomposition process, besides hydrogen, highly volatile products, involving borazine ($N_3B_3H_6$) and monomeric BH_2NH_2, are generated with different heating rates.[4] Currently, the slow dehydrogenation kinetics, irreversibility, and formation of volatile materials (trace borazine and ammonia) have limited its practical application.[5] To overcome these barriers, tremendous efforts have been devoted to developing new strategies to enhance the hydrogen storage properties of AB in solution and solid state such as the use of nanoscaffolds,[6,7] metallic catalysts,[8] and ionic liquids.[9] Another widely adopted approach is to manipulate the thermodynamics of the compound through substituting one or two H atoms in the NH_3 group by alkali metals or methane groups, e.g., forming $LiNH_2BH_3$,[10] $Ca(NH_2BH_3)_2$,[11] $MeNH_2BH_3$, and Me_2NHBH_3,[12] to improve the kinetics of the hydrogen release. Xiong et al.[13] recently reported the substitution of H by Li in AB using a ball-milling method, resulting in the release of hydrogen from $LiNH_2BH_3$ at ~90 °C. However, it is difficult to control the release of hydrogen during the synthesis of such materials by the method of ball-milling because the collision between the balls/wall and AB tends to induce decomposition.[13,14]

Simultaneously, recent works have proven that transitional metals such as Pd, Ir, and Ti complexes can catalyze AB dehydrogenation.[15,16] Manners and coworkers reported that the precious metals of Rh, Ir, and Ru catalyze AB dehydrogenation at room temperature with 0.5 mol % loading rate, at the same time suppressing the release of volatile cyclotriborazane (HN_2BH_2), borazine ($(HNBH)_3$), and poly(iminoborane) ($(HNBH)_n$).[17] They indicate that the early transition metallic metallocene complexes can act as highly active, homogeneous dehydrocoupling catalysts for Me_2HNBH_3.[8] Chen et al. examined Me_2HNBH_3 dehydrogenation using [Rh (1,5-cod) μ-Cl]$_2$ as a catalyst, and suggested that the presence of toluene-soluble Ru clusters and small amounts (<1%) of other rhodium species are functionalized for enhancing the hydrogen release rate from AB.[12] Heinekey and coworkers demonstrated significant efficacy of an iridium pincer complex [(pocop)Ir(H_2)] in the improvement of the dehydrogenation kinetics of AB,[18] while theoretical calculations by Paul and Musgrave[19] indicated the effects of polarity of AB and the importance of having both hydridic and acid hydrogen atoms in the same molecule on hydrogen release from AB. Although the controlled release of hydrogen from AB has been improved by metallic complex catalysts, the systems reported to date still face the following challenges: i) the release rate of hydrogen is not fast enough and the release temperature is higher than 80 °C; ii) the mechanism of dehydrogenation remains unclear; iii) the release of NH_3 is a problem; iv) it is desirable to replace the organic solvents, e.g., ether, THF, and diglyme, in catalytic dehydrogenation of AB systems.

It has been reported that materials structured at the nanoscale may enhance the kinetics or modify the thermodynamics of phase transitions and chemical reactions due to the effect of variation of surface energy with decreasing particle size,[20,21] introducing defects and vacancies, and shortening diffusion distance.[22] Confinement of materials within porous frameworks is hence a potentially viable approach to tune the thermodynamics of such materials for hydrogenation/dehydrogenation.[23,24] Insertion of AB into mesoporous silica or carbon cryogel has been demonstrated to significantly improve the kinetics and decrease the temperature for hydrogen release.[6,7]

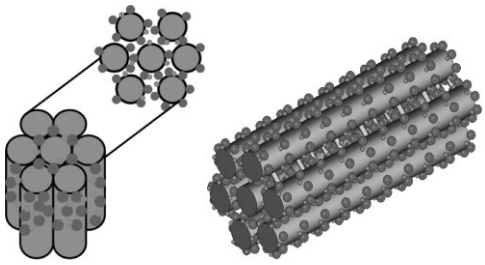

Figure 1. The schematic model of AB/CMK-3 and AB/Li^+-CMK-3 nanocomposites (dark gray balls: AB, light gray balls: Li, gray rod: CMK-3 substrate).

In this study, AB encapsulated within a mesoporous carbon (CMK-3) framework is studied in order to explore the potential for enhancement of hydrogen release by a nano-confinement effect. The system is further modified with a heterogeneous Li-based catalyst to accelerate the thermal decomposition of AB and suppress the volatile emissions, especially ammonia. The hierarchical structure of the AB/Li-CMK-3 framework is indicated schematically in Figure 1. The synthesis of the framework was carried out at room temperature to avoid significant decomposition of AB. The heterogeneous catalytic system for decomposition of AB in the solid state additionally avoids the need for volatile organic solvents. Two notable phenomena associated with this new AB system are expected: i) a synergetic effect of nanostructure confinement and Li catalysis that significantly enhances the dehydrogenation kinetics of AB; ii) the suppression of volatile products such as borazine and NH_3. A plausible mechanism of hydrogen release from the AB/Li-CMK-3 framework is suggested and discussed.

2. Results and Discussion

2.1. Characterization of AB/CMK-3 and AB/Li-CMK-3 Nanostructures

The ordered mesoporous carbon material used in this work, CMK-3, is characterized by large surface area, a uniform pore size, ordered pore structure, an interconnected pore network, and good thermal and mechanical stabilities.[25] This structure in principle allows for both high dispersion and high loading of hydrogen storage compounds and fine control of the compound clusters within nanochannel pores. The structure of the synthesized CMK-3 and the characterization by small angle X-ray diffraction (small angle XRD), scanning electron microscopy (SEM), and transmission electron microscopy (TEM) are illustrated in Figure S1 (Supporting Information), which features rod morphology and an ordered pore structure with a uniformed

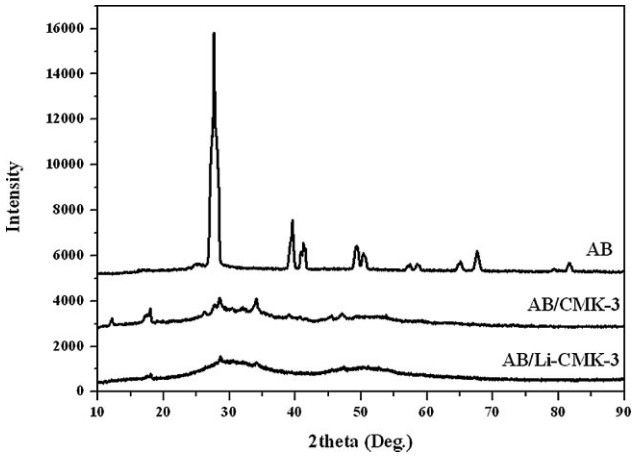

Figure 2. The XRD patterns of AB, AB/CMK-3, and AB/Li^+-CMK-3 samples.

pore diameter of 4.5 nm in 2D hexagonal geometry. The surface area and pore volume are around 1150 and 1.29 cm^3 g^{-1}, respectively.

The 50% AB/CMK-3 and 5% Li-doped AB/CMK-3 structures (AB: $C = 50{:}50$) were synthesized by an impregnation method. Because of the nanochannel nature of CMK-3 carbon, the AB and/or Li^+ saturated solutions were infiltrated rapidly into the internal channels of CMK-3 by a capillary effect. The XRD patterns in Figure 2 show a typical polycrystalline structure for pure AB with tetragonal lattice. The characteristic diffraction peaks of AB became broad with much weaker intensity after loading into CMK-3 and Li/CMK-3 frameworks, indicating that AB is highly dispersed on mesoporous CMK-3 at the nanoscale. The N_2 adsorption–desorption isotherms indicate that the surface area of CMK-3 was significantly reduced from 1 150 to 32.5 m^2 g^{-1} after AB and Li impregnation (see Figure S2 of the Supporting Information).

The structure of AB/CMK-3 frameworks was further studied by TEM with energy dispersive analysis by X-ray (TEM-EDX). The TEM and EDX element maps in Figure 3 confirm that the C map (in Fig. 3a) corresponds to the structure of CMK-3. The N and B maps in Figures 3b and c are observed to coincide very well with the C map, demonstrating the high dispersion of AB in the CMK-3 framework. The XRD and TEM-EDX results support the assertion that the AB was encapsulated into the channels of CMK-3, forming an embedded nanocomposite structure (as shown in Fig. 1). This nanophase may be anticipated to have modified surface energy in comparison with bulk AB, as well as defects that may favor to the cleavage of N–H and B–H bonds. Such features can clearly promote the easier release of hydrogen and enhanced dehydrogenation kinetics evidenced below.

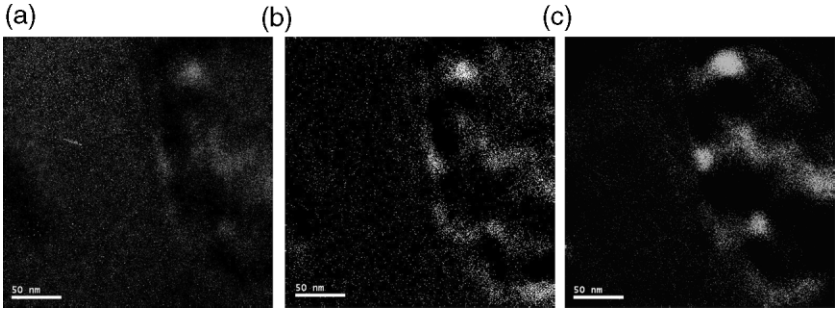

Figure 3. The EDX maps of C, N, and B elements in AB/CMK-3 nanocomposite.

2.2. Dehydrogenation

The hydrogen desorption profiles of AB and AB/CMK-3 measured by thermogravimetry combined with mass spectroscopy (TG/MS) are shown in Figures 4 and 5. It is evident that the neat AB starts to decompose at above 100 °C via a two-step process [i.e., reactions (1) and (2)] and the weight loss from the neat AB sample in Figure 4 reaches around 20 wt % below 150 °C with a heating rate of 1 °C min^{-1}. This is much larger than the theoretical hydrogen release capacity in AB via reactions (1) and (2) (13.4 wt % in total) due to the formation of volatile products other than hydrogen gas from AB, as is demonstrated by the MS characterization (Fig. 5). It is noteworthy that a small amount of NH_3 ($m/e = 17$) was observed as well as borazine ($m/e = 80$); these gases may poison the catalyst in PEM fuel cells and thus would have to be prevented in any practical application of AB as a hydrogen storage material.

Compared with the neat AB, the decomposition of AB/CMK-3 nanostructures occurs below 75 °C with only one-step for the release of gaseous substances. The weight loss of AB/CMK-3 approaches 27 wt % below 150 °C, which is even larger than that of the neat AB. Figure 5 also demonstrates that AB/CMK-3 releases hydrogen at a lower temperature with a desorption peak at 95 °C, while the neat AB at two release peaks around 110 and 145 °C. As described previously, AB was confined within the mesopores of CMK-3, resulting in the reduction of its size (~4.5 nm). This size reduction of AB leads to a short diffusion path for emitted hydrogen, which is likely to be one of the main factors enhancing the dehydrogenation kinetics. Furthermore, the acid property and functional groups on the surface of CMK-3 are likely to play important roles in the dehydrogenation kinetics and the decomposition pathways. As reported in our previous studies,[26] CMK-3 has acid functionality (pH = 3.7) with abundant hydroxyl and carboxyl groups on the surface (see Figure S3 of the Supporting Information), due to HF washing during the synthesis of CMK-3. The hydroxyl (–OH) and carboxyl (COOH) groups as proton donors can easily interact with the B–H hydridic hydrogen in AB to form an interface involving dihydrogen-like coordinated functionalities $–O–H\cdots H–BH_2NH_3$.[27,28] Such interactions can significantly influence the structure, reactivity, and selectivity in the solution and the solid state of AB. The formation of surface–$O–H\cdots H–BH_2NH_3$ can also be inferred from XRD results in which the peaks of AB on CMK-3 are shifted compared with those of AB (Fig. 2). When heating these materials, the hydrogen is released through the interaction between Lewis acidic and basic sites and form surface–$O–BH_2NH_3$ groups. A simplified mechanism of AB decomposition

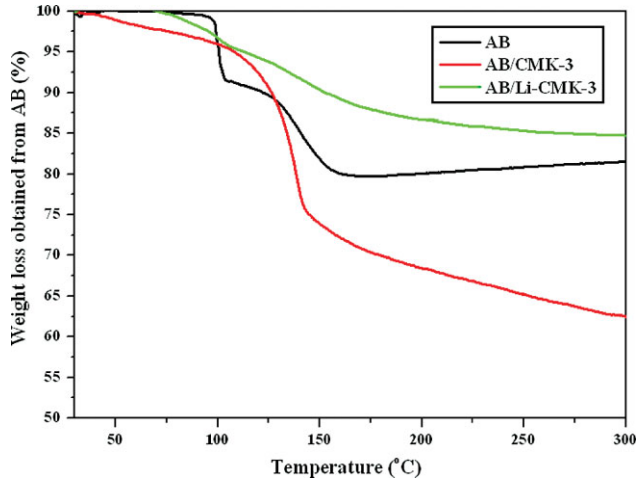

Figure 4. Hydrogen release from neat AB, AB/CMK-3, and AB/Li-CMK-3 measured by TG.

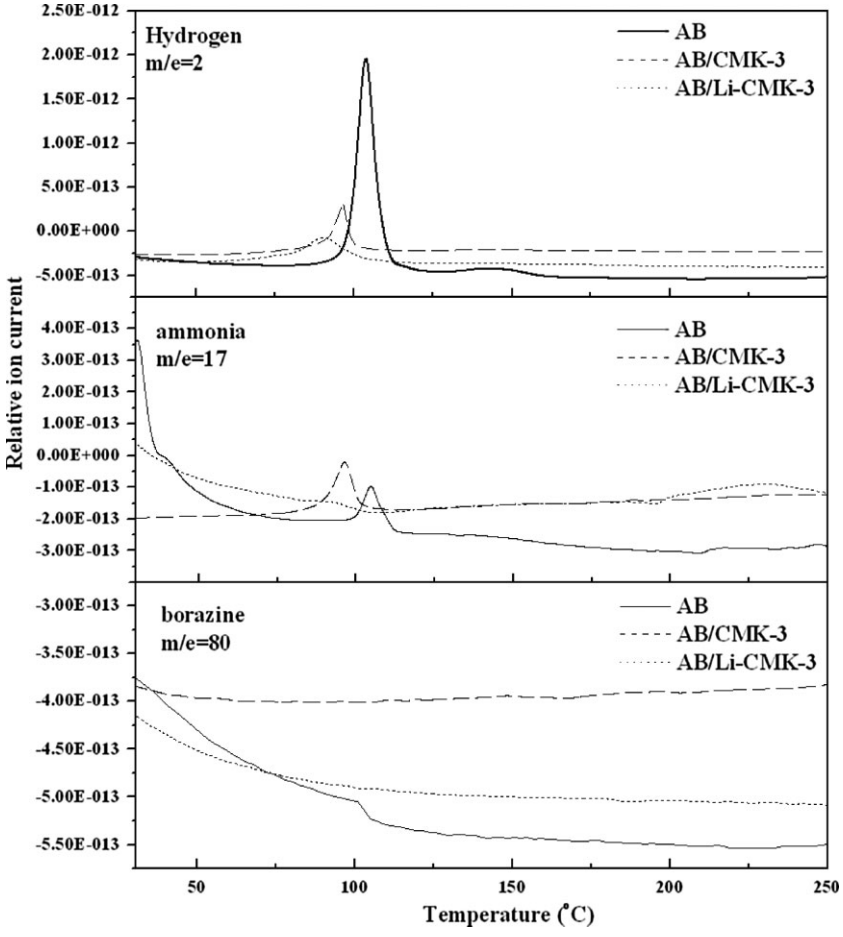

Figure 5. The MS results of AB, AB/CMK-3, and AB/Li^+-CMK-3.

on CMK-3 is suggested in Figure 6, in which the B–H hydridic hydrogen in AB as the electron donor can associate with the surface-OH groups in CMK-3 to form surface–O–H···· H–BH_2NH_3 structures, thereby destabilizing the network of AB. This can explain collectively: i) the enhancement of dehydrogenation, ii) a large amount of NH_3 release, and iii) borazine suppression when heating AB inside CMK-3. The phenomenon of hydrogen and ammonia release (caused apparently by the weak B–N interaction and was confirmed by the MS results in Fig. 5) influenced by the decomposition temperature was also noted by Custelcean et al.[28] in $NaCNBH_3$ and $NaBH_4$ with triethanolamine complex and by Epstein and coworkers[29] in organorhenium complex.

To further understand this mechanism, we investigated the thermodynamics of AB and AB/CMK-3 samples by differential scanning calorimetry (DSC) and the surface properties of AB/CMK-3 by X-ray photoelectron spectroscopy (XPS). Figure 7 shows the B 2 s XPS results of AB/CMK-3 before and after the decomposition. The peaks ~188.2 and ~192.0 eV in the XPS patterns are attributed to B–H and B–O bonds, respectively. The formation of B–O bonds suggest the interaction of AB and CMK-3 (B is from AB and O is from OH on the surface of CMK-3). When heating to 150 °C with a heating rate of 1 °C min^{-1}, the significant reduction of N content confirms the ammonia release during the AB/CMK-3 thermal decomposition. After the thermal decomposition, the intensity of B–O peaks is increased and no change of B content are observed, indicating boron immobilization on the carbon surface.

DSC results of AB and AB/CMK-3 in Figure 8 also illustrate that the decomposition reaction enthalpy from AB/CMK-3 ($\Delta H = -2.1$ kJ mol^{-1}) is significantly less than that from the neat AB ($\Delta H = -19.6$ kJ mol^{-1}),[6] indicating that the acid catalysis of hydroxyl and carboxyl groups leads to a change in the thermodynamics of thermal decomposition. This may be the reason that the AB inside CMK-3 can release hydrogen in one-step at a significantly lower temperature. Although borazine was suppressed by AB/CMK-3, in good agreement with the literature, as noted above a large amount of ammonia was detected from the AB decomposition in AB/CMK-3 (Fig. 5), which has not previously been reported. This is clearly detrimental and needs to be prevented for the target applications.

2.3. Catalytic Effect of Li Catalyst

To prevent ammonia release from AB/CMK-3, Li^+ was doped at the interface of AB and CMK-3 and then the thermal decomposition of AB/Li-CMK-3 was performed. The dehydrogenation properties of AB/Li-CMK-3 are also shown in Figures 4 and 5. The first notable phenomenon observed from the AB/Li-CMK-3 is that *only* H_2 gas was detected when heating up to 150 °C, which is indicative of complete suppression of ammonia and borazine release from AB. This suggests that the Li^+ plays an important role in nitrogen immobilization during the thermal decomposition. This is very

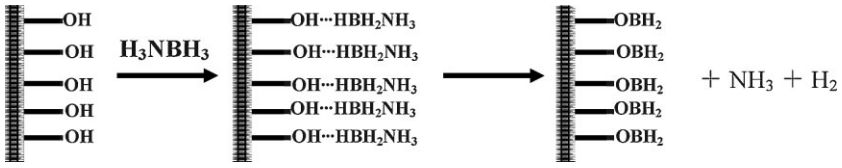

Figure 6. The mechanism of hydrogen release of AB/CMK-3 nanocomposite.

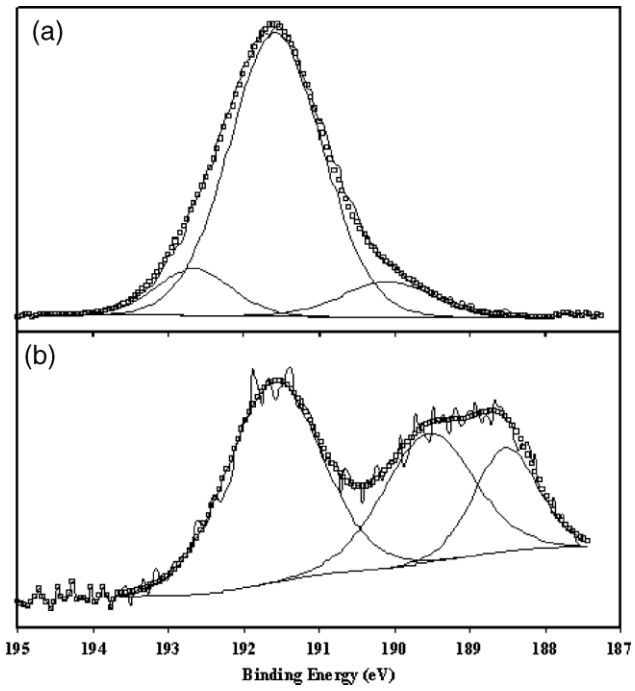

Figure 7. The B *1s* XPS results of AB/CMK-3 nanocomposite before A) and after B) thermal decomposition.

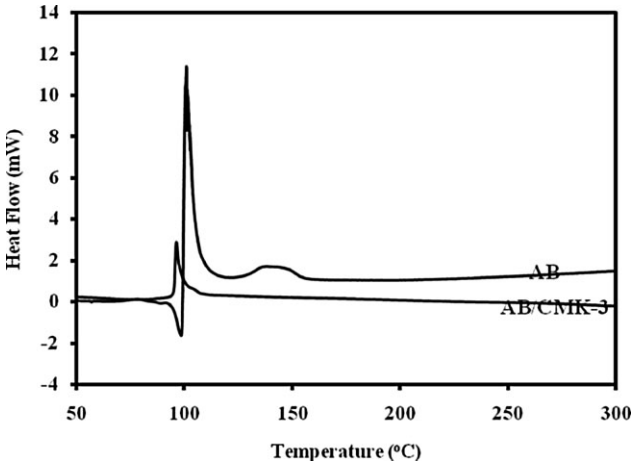

Figure 8. The DSC results of neat AB and AB/CMK-3 nanocmoposite.

important for AB thermal decomposition because NH_3 released from AB leads to a decrease of the hydrogen capacity of AB, reducing the capacity for reloading hydrogen and additionally poisoning the PEM fuel cell. More interestingly, hydrogen release of AB/Li-CMK-3 initially occurred at very low temperature around 55 °C with a broad peak at 90 °C (compared with AB/CMK-3 that started the decomposition at 75 °C with the desorption peak at 95 °C), indicating that the catalytic effect of the Li-based catalyst combined with the confinement of CMK-3 results in a further significant acceleration of dehydrogenation kinetics of AB within the Li-CMK-3 framework. It is apparent from Figures 4 and 5 that 11 wt % of hydrogen is released from AB/Li-CMK-3 when heating up to 150 °C, which is close to the theoretical hydrogen capacity of AB at a temperature below 150 °C. Therefore, the above results suggest that a synergistic interaction between catalyst and nanostructure can provide a very effective strategy to significantly accelerate the dehydrogenation kinetics and suppress the emission of ammonia from AB.

It is very important for the practical applications of AB to understand the mechanism of the thermal decomposition of AB within the Li-doped mesoporous CMK-3 framework. Ichikawa et al. investigated the mechanism of hydrogen desorption in a Li–N–H system and indicated that the NH_3 emission can be suppressed by a reaction with LiH during dehydrogenation.[30] This strategy was further confirmed to be effective in ball milled LiH and AB.[13,31] In this study, we doped Li^+ between the interface of AB and carbon by the pyrolysis of a $LiNO_3$ precursor. Consequently, Li^+ should be in the form of surface-O-Li on the surface of CMK-3 with the positive charge as reported in the literature.[32] Because of the electron donor property of NH_3, the positive surface-O-Li functionality may interact with NH_3 in the surface–O–H····H–BH_2NH_3 complex to form structures like surface–O–H····H–BH_2NH_3····Li-O-surface. Structures of this type would further weaken B–H and N–H bonds, offering an explanation for the accelerated hydrogen release from Li-doped AB/CMK-3. Although we have been unable to observe Li–N compounds by XRD, it is noteworthy that XPS results show no change of N content after the thermal decomposition until 300 °C. Therefore, in AB/Li-CMK-3, it appears that the main mechanistic function of Li^+ is to interact with and thereby fix NH_3 groups in AB, which prevents the release of ammonia during the AB decomposition. Li^+ is also functionalized to enhance the hydrogen release rate due to the formation of N–Li–O complexes. It is also suggested the combination of Li^+ and NH_3 during the decomposition of AB within Li-CMK-3 framework, based on the fact that the AB/Li-CMK-3 can release only 11 wt % hydrogen which is less than the theoretical capacity of ~13 wt % of hydrogen (Fig. 4).

To gain further insight into the hydrogen release of AB/Li-CMK-3, we investigated the dehydrogenation properties of AB/Li-CMK-3 nanostructures in isothermal models at different temperatures; the results of which are plotted in Figure 9. The AB within Li-CMK-3 framework can release ~7 wt % hydrogen at a very low temperature of 60 °C. The dehydrogenation rate is similar to that reported by Xiong et al.[13] but the operating temperature here is significantly lower. The activation energy for

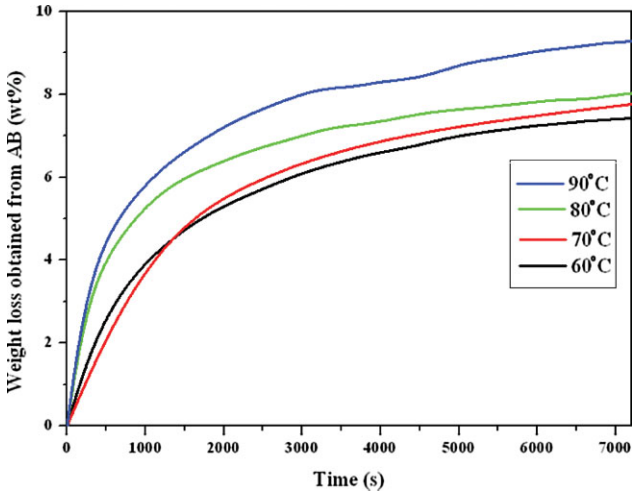

Figure 9. The gravimetrically measured H_2 release from AB/Li^+-CMK-3 nanocomposite.

the hydrogen release of this AB/Li-CMK-3 is determined to be $\sim 98 \pm 5$ kJ mol^{-1} (derived from Figure S4 of Supporting Information), which is remarkably lower than that of the neat AB (184 ± 5 kJ mol^{-1}),[6] thus providing direct evidence for the possibility of modifying the thermodynamics of the AB decomposition within the Li-CMK-3 frameworks. It should be noted that the amount of the released hydrogen from the *overall* AB/Li-CMK-3 composite material is ~3.5 wt % (due to the 50:50 ratio of AB and carbon). However, it is anticipated that this value can be significantly improved by optimization of the structure and pore volume of CMK-3[33] and the AB loading ratio.

Although we hope that the nano-confinement will modify the thermodynamics of the system that will benefit the reversibility of AB; however, no reversible phenomenon has been observed by current study. It should be noted that the confinement did change the thermodynamics of the AB decomposition, evidenced by the one-step reaction for hydrogen release in AB/CMK-3 system instead of the original two-step reactions of neat AB. This implies that the hypothesis should be re-explored in the future studies under different testing conditions, e.g., very high hydrogen pressure.

3. Conclusions

AB, within a Li-CMK-3 framework can release up to ~7 wt % hydrogen at a temperature as low as 60 °C, which would enable the release of hydrogen to be driven by the waste heat of PEM fuel cells. We have demonstrated that synergistic effects of nanostructure confinement and catalysis in the Li-CMK-3 system significantly accelerate the dehydrogenation kinetics of the AB loaded system and suppress the release of undesirable volatile products. The discovery of catalytic effect of noncovalently bound Li—as distinct from substituting H in the NH_3 group—on hydrogen release in AB appears very promising and implies a new mechanism that can be exploited for enhanced performance of AB materials in hydrogen storage.

4. Experimental

CMK-3 Synthesis: CMK-3 was prepared following the method reported by Ryoo et al.[34] using ordered mesoporous silica (SBA-15) as template. Successive two-step impregnation procedure and high temperature calcination at 900 °C under N_2 atmosphere were employed. The silica template was removed by 10% HF solution at room temperature and the carbon sample was washed with distilled water before drying in air at room temperature for 24 h.

AB/CMK-3 Synthesis: AB (500 mg) was dissolved in 15 mL CH_3OH and 500 mg CMK-3 was added to the solution with stirring. The solvent were removed under vacuum to obtain the solid AB/CMK-3 nanocomposite.

AB/Li-CMK-3 Synthesis: $LiNO_3$ (490 mg) and 950 mg CMK-3 were added to 30 mL CH_3CH_2OH with stirring for 2 h, and the mixture was dried at 50 °C in the oven. The dried sample was calcined at 750 °C under Ar flow gas to obtain 5% Li/CMK-3.

Characterization: The morphology and microstructure of the synthesize samples were characterized by XRD, N_2 absorption–desorption isotherms, TEM, and SEM. The thermoanalysis and decomposition process were determined by TG/MS. The XRD patterns of the samples were performed on a Rigaku MIniflex diffractometer with Co Kα radiation at a scanning rate of 2 ° min^{-1} in the 2θ range from 10 to 80 °. The BET surface areas and textural structure were measured using an automated adsorption analyzer (Autosorb-1C, Quantachrome, USA). TEM observation was conducted on a F20 microscope with an accelerating voltage 200 kV. The TEM samples were prepared by dipping ultrasonically dispersed the samples in ethanol on holey carbon grids. The SEM photomicrograph of the samples was taken in a JEOL 6300 microscope with Pt coating. The gaseous compositions from AB decomposition were determined by a coupled TG/MS technique. All thermal analyses were measured from room temperature to 300 °C at a heating rate of 1 °C min^{-1} under Ar gas flow. The XPS measurements were conducted using a PHI-560 ESCA system (PerkinElmer). All spectra were acquired at a basic pressure 2×10^{-7} torr with Mg Kα excitation at 15 kV and recorded in the ΔE = constant mode, at pass energies of 50 and 100 eV.

Acknowledgements

The financial support from the Australian Research Council and Shanghai Science Committee, SLADP (B108) are gratefully acknowledged. Supporting Information is available online from Wiley InterScience or from the corresponding authors.

Received: July 31, 2008
Revised: October 14, 2008
Published online: December 16, 2008

[1] L. Schlapbach, A. Zuttel, *Nature* **2001**, *414*, 353.
[2] M. G. Hu, R. A. Geanangel, W. W. Wendlandt, *Therochim. Acta* **1978**, *23*, 249.
[3] T. Autrey, A Gutowska, L.Y Li, M Gutowski, J Linehan, http://www.hydrogen.energy.gov/pdfs/review04/stp2autrey04.pdf, accessed August **2008**.
[4] F. Baitalow, J. Baumann, G. Wolf, K. Jaenicke-Rößler, G. Leitner, *Therochim. Acta* **2002**, *391*, 159.
[5] T. B. Marder, *Angew. Chem. Int. Ed.* **2007**, *46*, 8116.
[6] A. Gurowska, L. Y. Li, Y. S. Shin, C. M. Wang, X. S. Li, J. C. Linehan, R. S. Smith, B. D. Kay, B. Schmid, W. Shaw, M. Gutowski, T. Autrey, *Angew. Chem. Int. Ed.* **2005**, *44*, 3578.
[7] A. Feaver, S. Sepehri, P. Shamberger, A. Stowe, T. Autrey, G. Z. Cao, *J. Phys. Chem. B* **2007**, *111*, 7469.
[8] T. J. Clark, C. A. Russell, I. Manners, *J. Am. Chem. Soc.* **2006**, *128*, 9582.

[9] M. E. Bluhm, M. G. Bradley, R. Butterick, U. Kusari, L. G. Sneddon, *J. Am. Chem. Soc.* **2006**, *128*, 7748.
[10] M. Bowden, I Brown, K.I MacKenzie, http://www.iphe.net/Storage%20%20Lucca/postersPDFs/CH7%20BowdenMark%20IPHE%20Storage%20Lucca.pdf accessed May **2007**.
[11] H. V. K. Diyabalanage, R. R. Shrestha, T. A. Semelsberger, B. L. Scott, M. E. Bowden, B. L. Davis, A. K. Burrell, *Angew. Chem, Int. Ed.* **2007**, *46*, 8995.
[12] Y. Chen, J. L. Fulton, J. C. Linehan, T. Autrey, *J. Am. Chem. Soc.* **2005**, *127*, 3254.
[13] Z. T. Xiong, C. K. Yong, G. T. Wu, P. Chen, P. Shaw, A. Karkamkar, T. Autrey, M. O. Jones, S. R. Johnson, P. P. Edwards, W. I. F. David, *Nat. Mater.* **2008**, *7*, 138.
[14] S. De Benedetto, M. Carewska, C. Cento, P. Gislon, M. Pasquali, S. Scaccia, P. P. Prosini, *Therochim. Acta* **2006**, *441*, 184.
[15] I. G. Green, K. M. Johnson, B. P. Roberts, *J. Chem. Soc. Perkin Trans.* **1989**, *2*, 1963.
[16] C. A. Jaska, K. Temple, A. J. Lough, I. Manners, *Chem. Commun.* **2001**, 962.
[17] C. A. Jaska, K. Temple, A. J. Lough, I. Manners, *J. Am. Chem. Soc.* **2003**, *125*, 9424.
[18] M. C. Denney, V. Pons, T. J. Hebden, D. M. Heinekey, K. I. Goldberg, *J. Am. Chem. Soc.* **2006**, *128*, 12048.
[19] a) A. Paul, C. B. Musgrave, *Angew. Chem.* **2007**, *119*, 8301; *Angew. Chem. Int. Ed.* **2007**, *46*, 8153.
[20] M. J. Msyo, A. Suresh, W. D. Porter, *Rev. Adv. Mater. Sci.* **2003**, *5*, 100.
[21] C. P. Baldé, B. P. C. Hereijgers, J. H. Bitter, K. P. de Jong, *J. Am. Chem. Soc.* **2008**, *130*, 6761.
[22] X. D. Yao, C. Z. Wu, A. J. Du, J. Zou, Z. H. Zhu, P. Wang, H. M. Cheng, S. C. Smith, G. Q. Lu, *J. Am. Chem. Soc.* **2007**, *129*, 15650.
[23] R. W. P. Wagemans, J. H. Lenthe, P. E. Jongh, A. J. Dillen, K. P. Jong, *J. Am. Chem. Soc.* **2005**, *127*, 16675.
[24] R. W. P. Wagemans, J. H. Lenthe, P. E. Jongh, A. J. Dillen, K. P. Jong, *J. Am. Chem. Soc.* **2005**, *127*, 16675.
[25] S. H. Joo, S. J. Choi, I. Oh, J. Kwak, Z. Liu, O. Terasaki, R. Ryoo, *Nature* **2001**, *412*, 169.
[26] L. Li, Z. H. Zhu, G. Q. Lu, Z. F. Yan, S. Z. Qiao, *Carbon* **2007**, *45*, 11.
[27] R. Custelcean, J. E. Jackson, *Chem. Rev.* **2001**, *101*, 1963.
[28] R. Custelcean, J. E. Jackson, *J. Am. Chem. Soc.* **1998**, *120*, 12935.
[29] E. S. Shubina, N. V. Belkova, A. N. Krylov, E. V. Vorontsov, L. M. Epstein, D. G. Gusev, M. Niedermann, H. Berke, *J. Am. Chem. Soc.* **1996**, *118*, 1105.
[30] T. Ichikawa, N. Hanada, S. Isobe, H. Y. Leng, H. Fujii, *J. Phys. Chem. B* **2004**, *108*, 7787.
[31] X. D. Kang, Z. Z. Fang, L. Y. Kong, H. M. Cheng, X. D. Yao, G. Q. Lu, P. Wang, *Adv. Mater.* **2008**, *20*, 2756.
[32] Z. H. Zhu, G. Q. Lu, S. C. Smith, *Carbon* **2004**, *42*, 2509.
[33] A. H. Lu, W. C. Li, W. Schmidt, W. Kiefer, F. Schüth, *Carbon* **2004**, *42*, 2939.
[34] R. Ryoo, S. H. Joo, Kruk, M. M. Jaroniec, *Adv. Mater.* **2001**, *13*, 677.